Ring Currents as Probes of the Aromaticity of Inorganic Monocycles : P_5^-, As_5^-, S_2N_2, $S_3N_3^-$, $S_4N_3^+$, $S_4N_4^{2+}$, $S_5N_5^+$, S_4^{2+} and Se_4^{2+}

Frank De Proft,[a] Patrick W. Fowler,[b] Remco W. A. Havenith,[b] Paul von Ragué Schleyer,[c] Gregory Van Lier,[a] and Paul Geerlings*[a]

Abstract: Current-density maps were calculated by the ipsocentric CTOCD-DZ/6-311G** (CTOCD-DZ = continuous transformation of origin of current density-diamagnetic zero) approach for three sets of inorganic monocycles: S_4^{2+}, Se_4^{2+}, S_2N_2, P_5^- and As_5^- with 6 π electrons; $S_3N_3^-$, $S_4N_3^+$ and $S_4N_4^{2+}$ with 10 π electrons; and $S_5N_5^+$ with 14 π electrons. Ipsocentric orbital analysis was used to partition the currents into contributions from small groups of active electrons and to interpret the contributions in terms of symmetry- and energy-based selection rules. All nine systems were found to support diatropic π currents, reinforced by σ circulations in P_5^-, As_5^-, $S_3N_3^-$, $S_4N_3^+$, $S_4N_4^{2+}$ and $S_5N_5^+$, but opposed by them in S_4^{2+}, Se_4^{2+} and S_2N_2. The opposition of π and σ effects in the four-membered rings is compatible with height profiles of calculated NICS (nucleus-independent chemical shifts).

Keywords: aromaticity · density functional calculations · inorganic monocycles · nucleus independent chemical shifts · ring currents

Introduction

Aromaticity, an essential term in the working vocabulary of organic chemistry,[1] has been used in thousands of papers[2] to rationalise stability, patterns of reactivity, reaction mechanisms and physical properties of delocalised ring systems.

One conventional measure of aromaticity is the ability of a system to sustain a diatropic ring current,[3] often diagnosed by calculation of the nucleus-independent chemical shift (NICS)[4] at or near the ring centre. Other criteria, from more traditional structural and energetic[5a,b] to recent conceptual DFT-based measures,[5c,d] and their application are discussed at length in reference [1e]. There is a long tradition of extension of the aromaticity concept to the domain of inorganic chemistry to help clarify the electronic structure of species such as borazine,[4b,6a] deltahedral boranes[6b,c] and pnictogen rings and clusters.[4b,6d] A striking recent development is the identification of "all-metal aromatics", in which the rings involve only metal atoms.[7] All these extensions carry implications about the ring currents to be expected in purely inorganic rings.

Modern theoretical methods allow direct visualisation of the current density induced by a magnetic field, and distributed-gauge mapping techniques[8] have been applied to many polycyclic organic[9] and some inorganic species.[10] The current-density map shows, for example, that borazine, the "inorganic benzene," is in fact nonaromatic according to this magnetic criterion,[9a] whereas 2π-electron Al_4^{2-} has a ring current, but of σ origin.[10a] We use the ipsocentric[9d] distributed-gauge method here to visualise the ring current, analyse its orbital origin and hence probe aromaticity in a number of simple inorganic rings that are accessible experimentally.[11a] Comparison is also made with NICS calculations. The species considered are P_5^-, As_5^-, S_2N_2, $S_3N_3^-$, $S_4N_3^+$, $S_4N_4^{2+}$, $S_5N_5^+$, S_4^{2+} and Se_4^{2+}.

The first series consists of P_5^- and As_5^-.[11b] P_5^-, the all-phosphorus analogue of the cyclopentadienide anion Cp^-, has been isolated in alkali metal salts[11c] and has been incorporated in several mixed sandwich complexes, for example, $[(\eta^5\text{-}C_5Me_5)Fe(\eta^5\text{-}P_5)]$, $[(\eta^5\text{-}C_5Me_5)_2Fe_2(\eta^5\text{-}P_5)]$ and $[(\eta^5\text{-}C_5Me_5)_2Cr_2(\eta^5\text{-}P_5)_2]$.[11d] Recently, the carbon-free sandwich complex $[(\eta^5\text{-}P_5)_2Ti]_2^-$ was prepared and characterised.[11e] Sandwich complexes containing As_5^- are also known.[11b,f] Previous theoretical studies showed that P_5^- is almost as aromatic as Cp^-.[11g] Recently, the electronic structures of X_5^- (X = P, As, Sb and Bi) were investigated by a combination of

[a] Prof. F. De Proft, Dr. G. Van Lier, Prof. P. Geerlings
Eenheid Algemene Chemie (ALGC)
Vrije Universiteit Brussel (VUB), Faculteit Wetenschappen
Pleinlaan 2, 1050 Brussels (Belgium)
Fax: (+32) 2-6293317
E-mail: pgeerlin@vub.ac.be

[b] Prof. P. W. Fowler, Dr. R. W. A. Havenith
School of Chemistry, University of Exeter
Stocker Road, Exeter EX44QD (UK)

[c] Prof. P. v. R. Schleyer
Department of Chemistry, University of Georgia
Athens, GA 30602 (USA)

Supporting information for this article is available on the WWW under http://www.chemeurj.org/ or from the author.

DOI: 10.1002/chem.200305291

photoelectron spectroscopy and ab initio calculations. All were found to have D_{5h} structures with nearby, but higher lying, C_{2v} isomers. On the basis of energetic arguments and analysis of the molecular orbitals, these compounds are all thought to be aromatic, although their valence MO ordering differs from that in Cp^-.[6d]

Our second series comprises four charged sulfur–nitrogen rings, typical of a large number of SN compounds which have been characterised experimentally.[11a,h] The cage compound S_4N_4, prepared by the reaction of NH_3 and S_2Cl_2 or SCl_2, is the main precursor for the preparation of other SN compounds.[11a,h] Thermal decomposition of S_4N_4 over Ag wool yields the unstable S_2N_2, which has a square-planar ring (D_{2h}) and is isoelectronic with S_4^{2+} (vide infra).[10a,h] $S_3N_3^-$ is formed when S_4N_4 is treated with azides or with potassium metal.[11i] Reaction of $S_3N_2Cl_2$ with S_2Cl_2 produces a salt containing the $S_4N_3^+$ ion.[11a,h] Oxidation of S_4N_4 with AsF_5 or SbF_5 yields the salts $[S_4N_4^{2+}](EF_6^-)_2$ (E = As or Sb).[11a,h,j] Depending on the counteranion, $S_4N_4^{2+}$ can adopt planar structures, either with equal bond lengths or with alternating distances and different angles at S and N, or nonplanar boat-shaped forms.[11a,h,] We also considered the 14 π-electron azulene-like isomer of the $S_5N_5^+$ ion.[11a,h,k]

The square-planar chalcogen dications S_4^{2+} and Se_4^{2+} also have been characterised in detail.[11a,l] These species are obtained as salts by selective oxidation of the elements with SbF_5 or AsF_5 in liquid HF or with $S_2O_2F_2$ in HSO_3F. Their bond lengths are about 3% shorter than typical E–E single bonds.[11a,l] Along with the isoelectronic, neutral four-membered ring S_2N_2, these constitute our third series.

We find that each of these ring systems supports a strong π diatropic current, as expected from the presence of $4n+2$ π electrons. However, the σ electrons of these inorganic rings also give rise to significant ring-current effects, which can reinforce or oppose the diatropicity of the π electrons, and have analogues in the diatropic "σ aromaticity" of cyclopropane and the paratropic ring-current activity of cyclobutane, ascribed on the basis of NICS analysis.[12] The different roles of σ and π electrons are explained by an ipsocentric orbital model that gives a clear rationale for the sense of rotation of the current and the number of electrons involved in producing that current.

Method

Optimised geometries of S_4^{2+}, Se_4^{2+}, P_5^-, As_5^-, S_2N_2, $S_3N_3^-$, $S_4N_3^+$, $S_4N_4^{2+}$ and $S_5N_5^+$ (Scheme 1) were obtained at the B3LYP/6-311+G** DFT level by using Gaussian 98.[13] All but $S_3N_3^-$ and $S_5N_5^+$ have planar minima, as confirmed by diagonalisation of the Hessian matrix. The D_{3h} structure of $S_3N_3^-$ has a single imaginary frequency and relaxes to a C_{3v}-symmetric minimum. The planar azulene-like C_{2v} structure of $S_5N_5^+$ considered here has a single imaginary frequency; it relaxes to nonplanar C_1 symmetry on full optimisation, but this form was not analysed further.

Current-density maps for all molecules in their planar geometries were calculated at the coupled Hartree–Fock level in the 6-311G** basis by using the distributed-origin method of Keith and Bader,[8a–b] as developed by the Modena group[8c–d] and implemented in the SYSMO program.[14] The diamagnetic zero (DZ) variant of the CTOCD (continuous transformation of origin of current density) method, in which the current density at each point in space is calculated with that point as origin, was used.

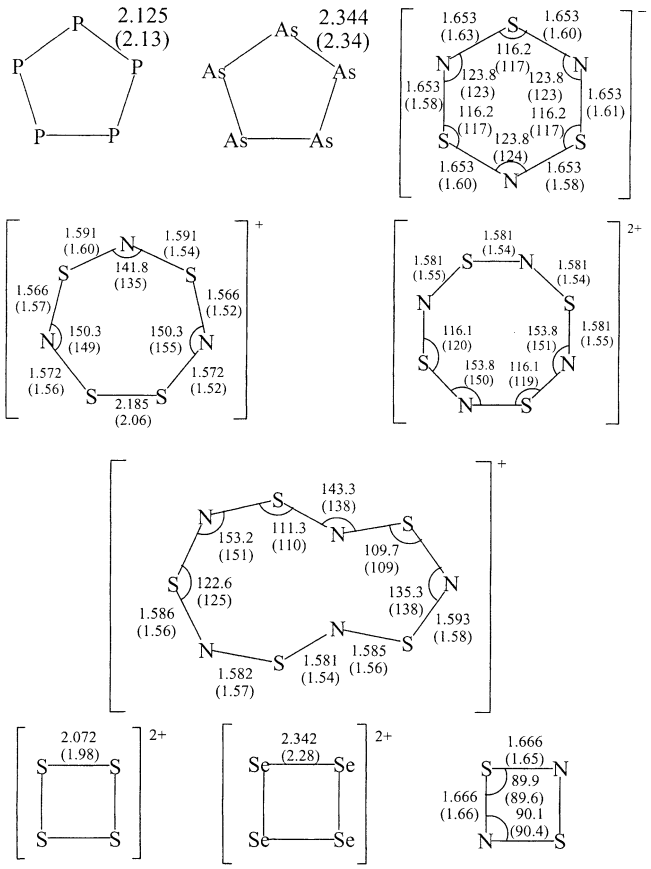

Scheme 1. Selected geometrical parameters of P_5^- (D_{5h}), As_5^- (D_{5h}), S_2N_2 (D_{2h}), $S_3N_3^-$ (D_{3h}), $S_4N_3^+$ (C_{2v}), $S_4N_4^{2+}$ (D_{4h}), S_4^{2+} (D_{4h}), Se_4^{2+} (D_{4h}) and $S_5N_5^+$ (C_{2v}), obtained at the B3LYP/6–311+G** level. Calculated bond lengths and angles are compared with experimental values (in parentheses).[10a] In the case of P_5^- and As_5^- the bond lengths are compared with the CCSD(T)/6-311+G** values, taken from ref. [5c]

This choice of an ipsocentric[9d] origin of vector potential has all the usual advantages of distributed-origin approaches: superior convergence with basis-set size and physically realistic[9e,f] current maps with modest basis sets. It also provides a specific partition of the first-order wavefunction, and therefore of the induced current density, into nonredundant orbital contributions that involve only occupied-to-virtual transitions and obey simple symmetry-based selection rules.[9c,d] This simplicity proves crucial for the interpretation of the results. In a π system subjected to a perpendicular magnetic field, nonvanishing orbital contributions arise only from transitions that are induced either by linear momentum operators that span the symmetry of in-plane translations, or by an angular momentum operator that has the symmetry of a rotation about the field direction. Expressed with respect to the molecular centre, the contributions of the first type are diamagnetic (diatropic), and those of the second are paramagnetic (paratropic). The terms diamagnetic and paramagnetic describe a circulation by its accordance with or opposition to Lenz's law; diatropicity and paratropicity refer to its effect on chemical shift of a test (and, in the present case, fictitious) nucleus.

In the maps, current densities induced by a magnetic field of unit strength acting along the principal axis are plotted in a plane parallel to that of the central ring. Contours denote the modulus of the current density at values $0.001\times4^n eh/2\pi m_e a_0^4$, and the vectors represent the in-plane projection of the current. A cutoff is applied to remove the very large vectors that arise in the vicinity of the nuclei for plots in the molecular plane. In all plots, diamagnetic circulation is counterclockwise and paramagnetic circulation clockwise. For carbon-based rings, maps have usually been plotted for a height of $1a_0$, which is close to the maximum of π charge and current densities, and leads to current that is essentially perpendicular to the inducing field. For each system in the present paper, we

plot the total ($\sigma + \pi$) current density in two planes: at a height h where the π current is close to maximal, and in the molecular plane, where the π contribution is vanishing due to symmetry. The height at which the π current density reaches its maximum strength was estimated from side-view plots of the π current density to be about $1\,a_0$ above the molecular plane for species containing only second-row elements, and about $1.5\,a_0$ above the plane for species including third-row elements. The side views also confirmed the current at these heights to be essentially parallel to the molecular plane in each case. The analysis of the total density into orbital contributions is illustrated for each system and shows currents arising from active π orbitals in plots at height h, as well as those arising from active σ orbitals in this or the molecular plane, depending on the system. Schematic energy-level diagrams are given to illustrate the application of the selection rules.

To indicate the effects of the currents shown in the maps on integrated molecular properties, NICS values were calculated at ring centres (NICS(0)) and at a height of 1 Å (NICS(1)). Comparison of the isotropically averaged NICS value at these two heights is one way of estimating relative contributions of σ and π electrons to this property, and by inference, to the ring current itself. Since the σ effects should fall off more rapidly with height from the ring centre, total NICS(1) values are often good indicators of the π effects.[4b,12b,5c,15] These results are reported in Table 1 for all nine species considered in the current-density maps.

Other methods for making such a separation include the "dissected localised NICS"[4b,12] (LMO-NICS) method, in which the Pipek–Mezey orbital localization scheme[16] is used in conjunction with the SOS-DFPT[17] method at the PW91/IGLOIII level.[18,19]

Table 1. Compilation of NICS values [ppm], calculated at the geometrical ring centre (NICS(0)) and 1 Å above it (NICS(1)).

Molecule	NICS(0)	NICS(1)
P_5^- D_{5h}	−18.5	−18.3
As D_{5h}	−20.5	−19.5
$S_3N_3^-$ D_{3h}	−14.9	−10.0
$S_4N_3^+$ C_{2v}	−12.1	−10.7
$S_4N_4^{2+}$ D_{4h}	−20.6	−17.0
$S_5N_5^{2+}$ C_{2v}	−18.9	−16.0
S_2N_2 D_{2h}	−2.6	−4.7
S_4^{2+} D_{4h}	−10.6	−7.9
Se_4^{2+} D_{4h}	−9.8	−7.6

Results and Discussion

P_5^- and As_5^-: In the ground state, P_5^- has a planar D_{5h} geometry.[6c] Figure 1 shows the calculated maps for the current density induced in this molecule by a perpendicular magnetic field. At a height of $1.0\,a_0$ (Figure 1a), the map shows an apparently classic example of a diatropic ring current, but in fact this feature persists all the way down to the molecular plane (Figure 1b) and so is not solely a conventional π current. The orbital analysis explains these two features. The current density at $1.0\,a_0$ has approximately equal contributions from the four electrons in the $2e_1''$ HOMO (π, Figure 1c) and the four in the $6e_2'$

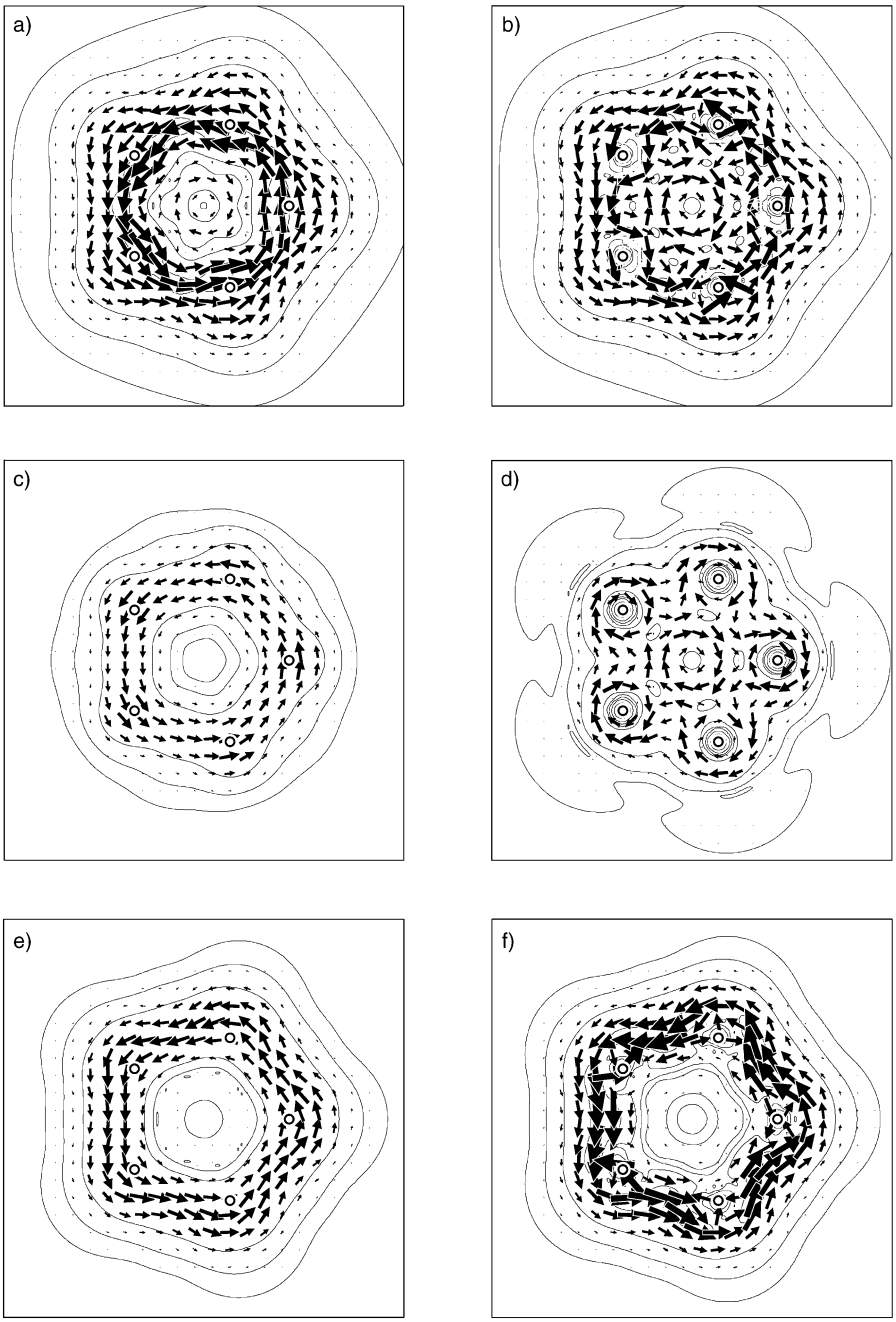

Figure 1. Calculated current-density maps and orbital contributions to ring current for P_5^-: a) total ($\sigma+\pi$) current density plotted at a height of $1.0\,a_0$; b) total current density in the molecular plane; c) π current density arising from the four electrons of the $2e_1''$ HOMO (at height $1.0\,a_0$); d) current density arising from the four electrons of the σ $6e_1'$ HOMO−1 (molecular plane); e) current density arising from the four electrons of the σ $6e_2'$ HOMO−2 (at height $1.0\,a_0$); f) current density arising from the four electrons of the σ $6e_2'$ HOMO−2 (molecular plane).

HOMO-2 (σ, Figure 1e). The HOMO-1 $6e_1'$ electrons contribute an additional small net paratropic current at this height. In the molecular plane, the π current vanishes, and the current from $6e_2'$ (Figure 1f) remains as a strong diatropic circulation at the molecular periphery. In the interior of the ring, localised paratropic eddies are contributed by the HOMO-1 $6e_1'$ (Figure 1d). The diatropic sense of the HOMO and HOMO-2 and the paratropic sense of the HOMO-1 currents follow from the translational and rotational selection rules of the ipsocentric model (Figure 2).

The corresponding maps for As_5^- (Figure 2) show a similar pattern of currents and orbital contributions, which follow from the match in frontier orbital symmetries. Thus, these two inorganic rings are both like and unlike the carbon homologue in their aromaticity. Both X_5^- systems sustain a π current that has the diatropic sense and the four-electron character expected of a 6π analogue of the cyclopentadienyl anion, but with a flat NICS height profile (see Table 1) that indicates cooperation of σ electrons in the overall diatropicity of the current density pattern.

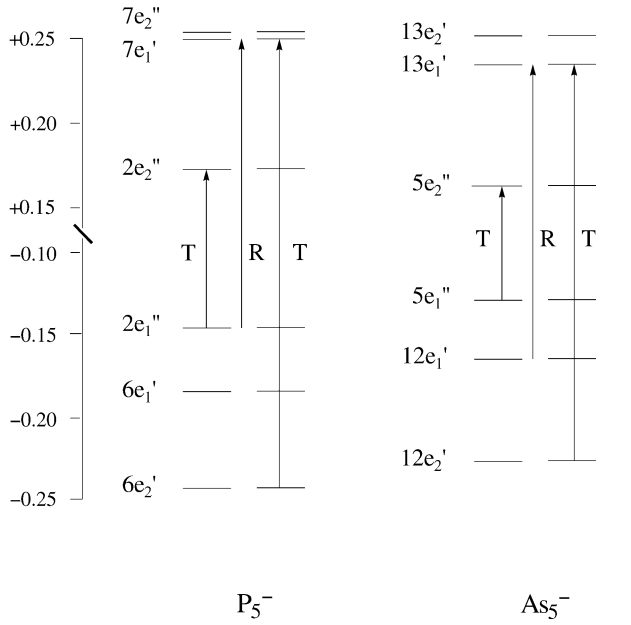

Figure 2. Energy-level diagrams and important translationally (T) and rotationally (R) allowed transitions leading to diatropic and paratropic currents for P_5^- and As_5^-.

$S_3N_3^-$, $S_4N_3^+$ and $S_4N_4^{2+}$: These three 10π-electron systems all show marked diatropic ring currents (Figures 3–5, Table 1). Analysis of MO contributions indicates that the current density can be attributed mainly to the four HOMO electrons in each case. The HOMO–LUMO excitation is translationally allowed; this ultimately derives from the ($\Lambda=2$)→($\Lambda=3$) transition of the idealised monocyclic ring,[9c] in which the orbital angular momentum jumps by one unit, consistent with an electric-dipole transition. In the D_{3h} point group of planar $S_3N_3^-$, the $\Lambda=2$ HOMO remains degenerate, as an e″ pair. In the C_{2v} and D_{4h} point groups the HOMO is split into $a_2 + b_1$ and $b_{1u} + b_{2u}$, respectively. The translationally (rotationally) allowed excitations, producing diatropic (paratropic) currents, are: in D_{3h}, e″→a_1'', a_2'', e″ (e″); in C_{2v}, $a_2 + b_1 \rightarrow a_2 + b_1$ ($a_2 + b_1$); in D_{4h}, $b_{1u} + b_{2u} \rightarrow e_g$ ($b_{1u} + b_{2u}$). The main active transitions for all three systems are marked on energy level diagrams in Figure 6. In all cases the nodal character of HOMO and LUMO inherited from the idealised monocycle ensures that the translational excitations dominate.

The σ electrons contribute localised diamagnetic circula-

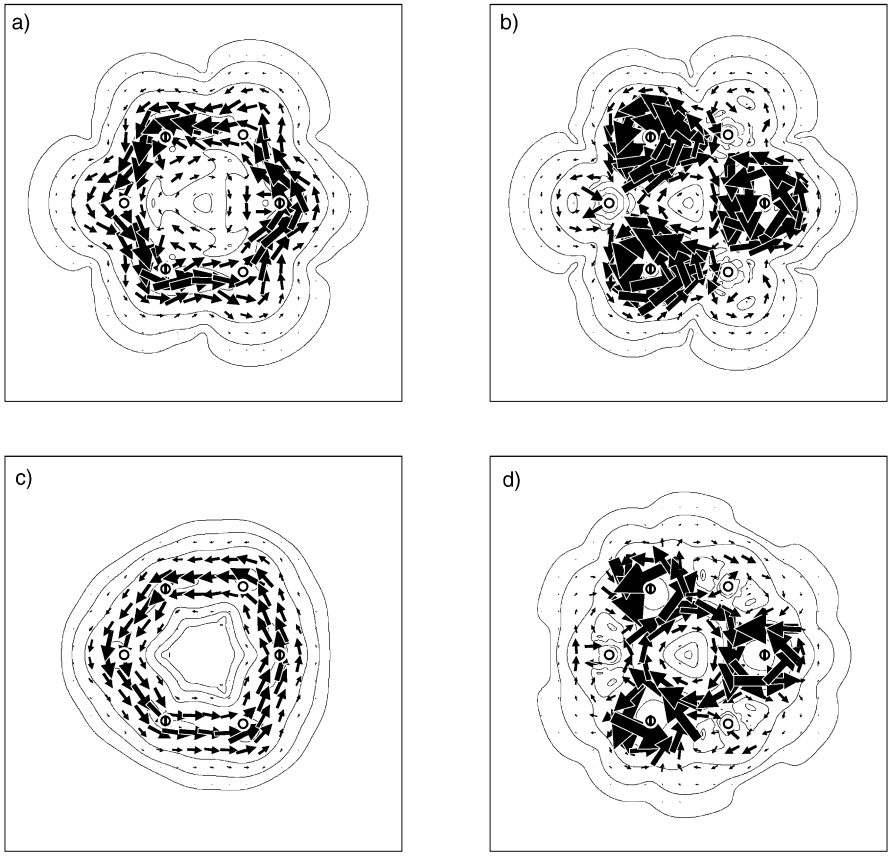

Figure 3. Calculated current-density maps and orbital contributions to ring current for $S_3N_3^-$: a) total (σ+π) current density plotted at a height of $1.0\,a_0$; b) total current density in the molecular plane; c) π current density arising from the four electrons of the 3e″ HOMO (at height $1.0\,a_0$); d) current density arising from the four electrons of the σ 9e′ HOMO−1 (molecular plane). Nitrogen centres are represented by a barred circle, and sulfur centres by an open circle.

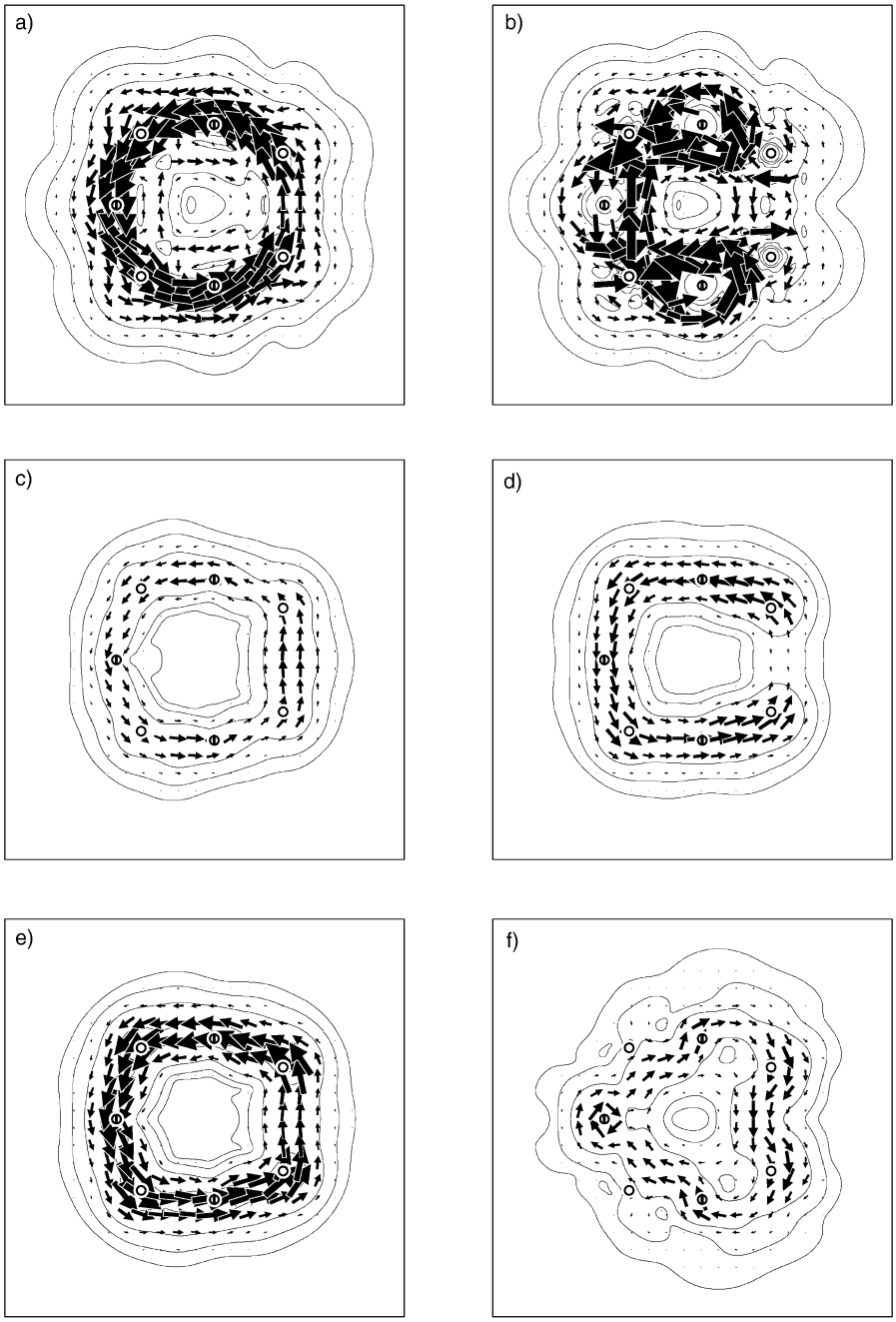

Figure 4. Calculated current-density maps and orbital contributions to ring current for $S_4N_3^+$: a) total ($\sigma+\pi$) current density plotted at a height of $1.0\,a_0$; b) total current density in the molecular plane; c) π current density arising from the two electrons of the $5b_1$ HOMO (at height $1.0\,a_0$); d) π current density arising from the two electrons of the $4a_2$ HOMO-1 (at height $1.0\,a_0$); e) total π current density (at height $1.0\,a_0$); f) current density arising from the two electrons of the σ $18a_1$ HOMO-2 (at height $1.0\,a_0$). Nitrogen centres are represented by a barred circle, and sulfur centres by an open circle.

tions on the N sites of all three rings, with maximal strength in the plane, but these do not constitute coherent ring currents. The sum of these localised circulations necessarily gives rise to a net paratropic circulation at the centre of the ring, which can be observed as a small inner feature of total current density in the out-of-plane plot for $S_3N_3^-$ (Figure 3a). The diatropic π current is strongest in $S_4N_4^{2+}$. In $S_4N_3^+$, the π current is less uniform than in the other two molecules, and is weakest in the long S–S bond, where the $4a_2$ component of the HOMO has a node. These trends are compatible with the NICS(0) and NICS(1) values reported in Table 1.

All three $S_xN_y^q$ systems sustain a π current with the diatropic sense and four-electron character expected of a planar $10\,\pi$-electron monocycle. All three systems are 4e diamagnetic in the terminology of reference [9c]. Apparently, the localised character of the energetically disparate S and N lone pairs prevents their contributing to a global current.

In the orbital picture, similar results can be expected for the next $4n+2$ π system, the $14\,\pi$-electron $S_5N_5^+$, in a planar geometry. As Figure 7 shows, this ring sustains a 4e diamagnetic π current arising from $\Delta\Lambda=+1$ transitions of the near-degenerate $7b_1$ HOMO and $5a_2$ HOMO-1 orbitals. The σ electrons contribute in-plane localised diamagnetic circula-

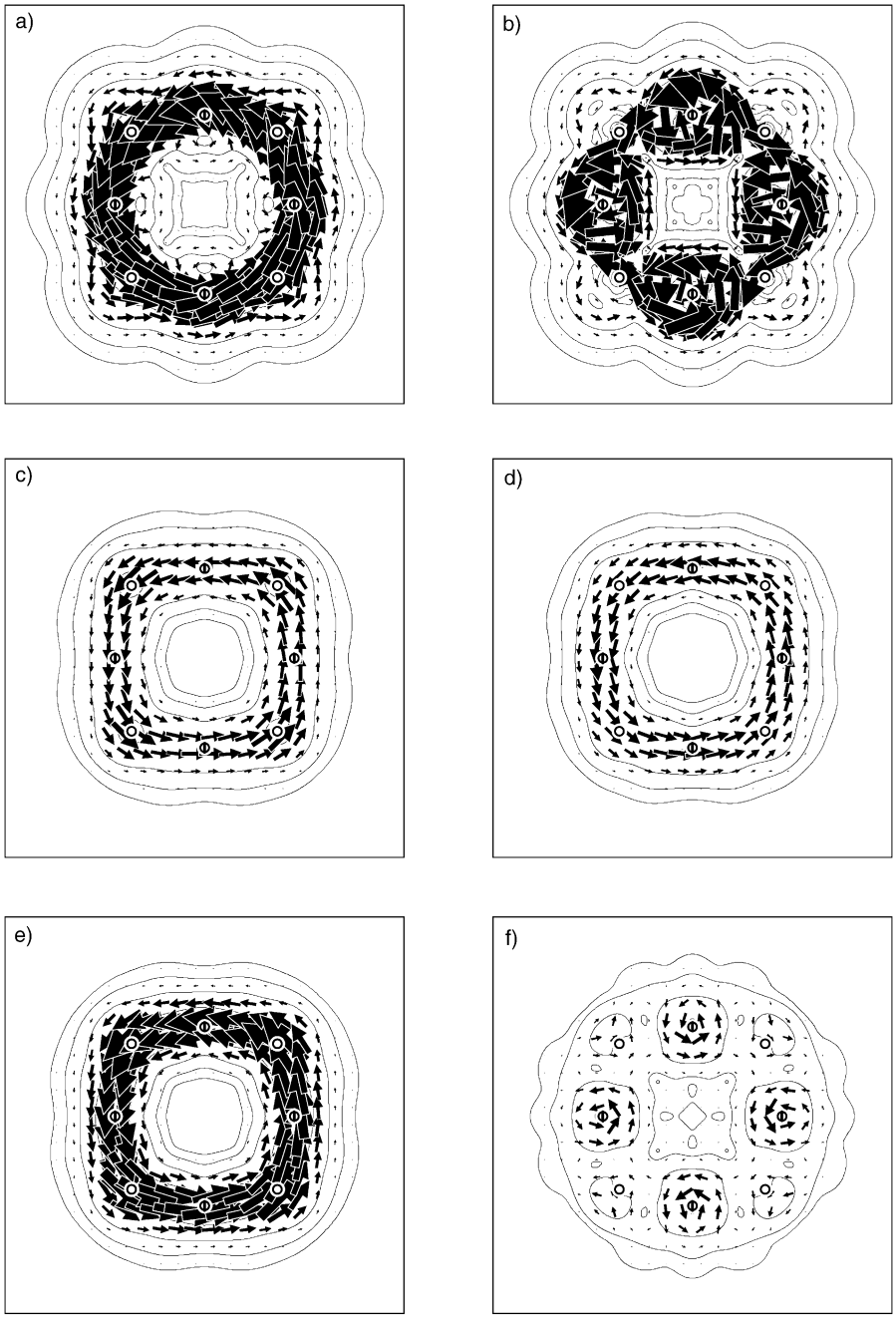

Figure 5. Calculated current-density maps and orbital contributions to ring current for $S_4N_4^{2+}$: a) total ($\sigma+\pi$) current density plotted at a height of $1.0\,a_0$; b) total current density in the molecular plane; c) π current density arising from the two electrons of the $2b_{1u}$ HOMO (at height $1.0\,a_0$); d) π current density arising from the two electrons of the $1b_{2u}$ HOMO-1 (at height $1.0\,a_0$); e) Total π current density (at height $1.0\,a_0$); f) current density arising from the four electrons of the σ $9e_u$ HOMO-3 (at height $1.0\,a_0$). Nitrogen centres are represented by a barred circle, and sulfur centres by an open circle.

tions on the nitrogen centres, as in the other members of the series. Comparison of NICS(0) and NICS(1) values (Table 1) indicates dominance of the diatropic π components.

S_4^{2+}, Se_4^{2+} and S_2N_2: The two X_4^{2+} 6π-electron systems show similar patterns of total ($\sigma+\pi$) current density in the out-of-plane maps (Figures 8 and 9). In both cases, the current is dominated by a peripheral diatropic circulation which encloses a paratropic central feature. The π contributions to the ring current in these dications arise from the four HOMO electrons through a translationally allowed transition to the π^* LUMO ($e_g \rightarrow b_{2u}$; Figure 10). The central paramagnetic feature is contributed by σ electrons, and hence has maximum strength in the molecular plane (Figure 11).

This feature arises as a result of partial cancellation between an inner paratropic current from the HOMO-1 e_u pair, and an outer diatropic current that runs in and out over the edges of the X_4 square and arises from the

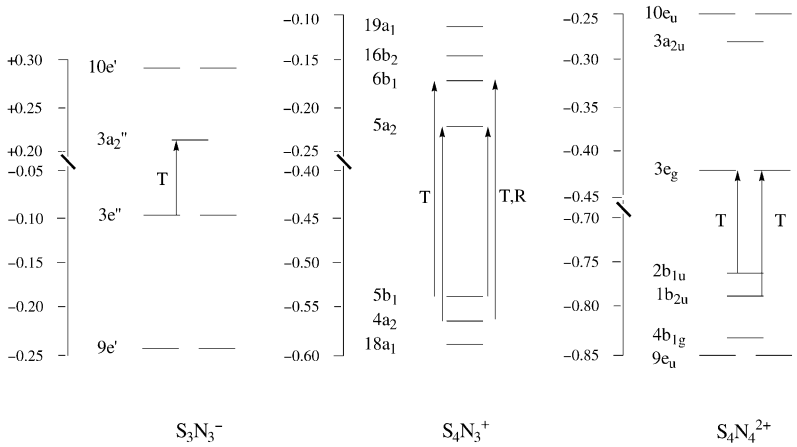

Figure 6. Energy-level diagrams and important translationally (T) and rotationally (R) allowed transitions leading to diatropic and paratropic currents for $S_3N_3^-$, $S_4N_3^+$ and $S_4N_4^{2+}$.

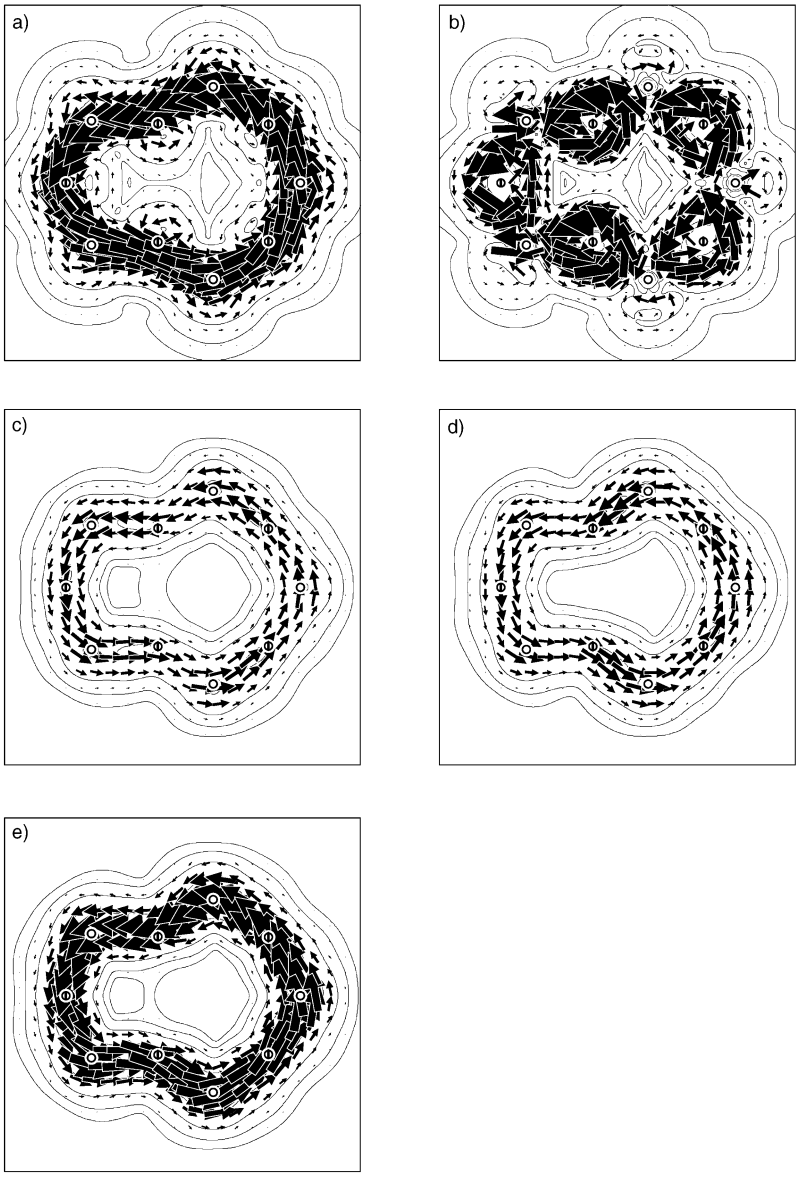

Figure 7. Calculated current-density maps and orbital contributions to ring current for $S_5N_5^+$: a) total ($\sigma+\pi$) current density plotted at a height of $1.0\,a_0$; b) total current density in the molecular plane; c) π current density arising from the two electrons of the $7b_1$ HOMO (at height $1.0\,a_0$); d) π current density arising from the two electrons of the $5a_2$ HOMO− (at height $1.0\,a_0$); e) total π current density (at height $1.0\,a_0$). Nitrogen centres are represented by a barred circle, and sulfur centres by an open circle.

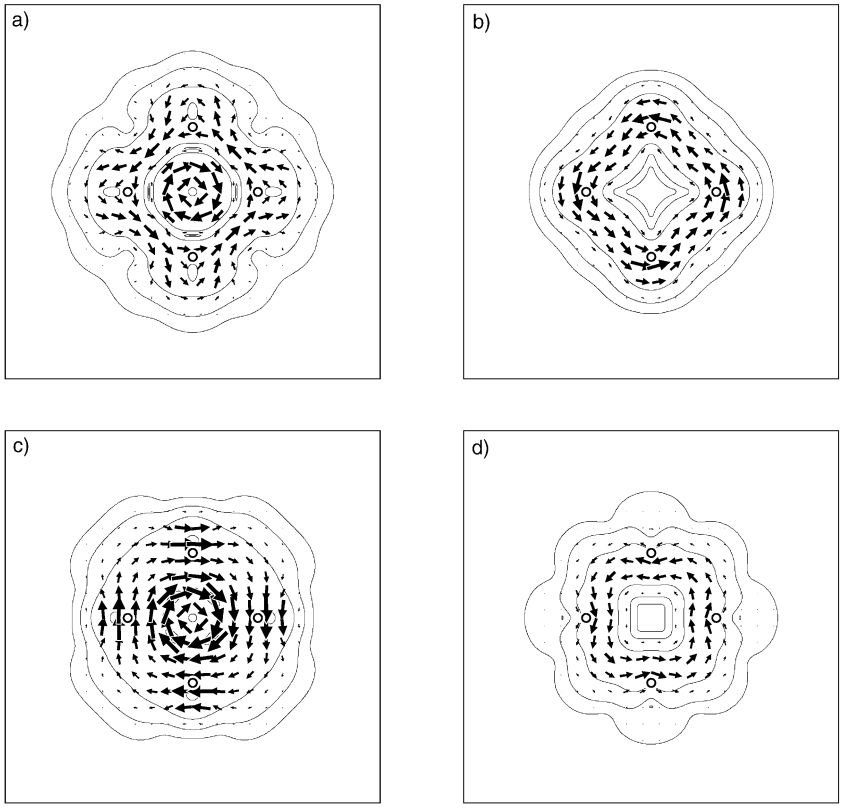

Figure 8. Calculated current-density maps and orbital contributions to ring current for S_4^{2+} in a plane at a height of $1.0\,a_0$: a) total current density; b) π current density arising from the four electrons of the $2e_g$ HOMO; c) current density arising from the four electrons of the σ $6e_u$ HOMO−1; d) current density arising from the two electrons of the σ $2b_{2g}$ HOMO−4.

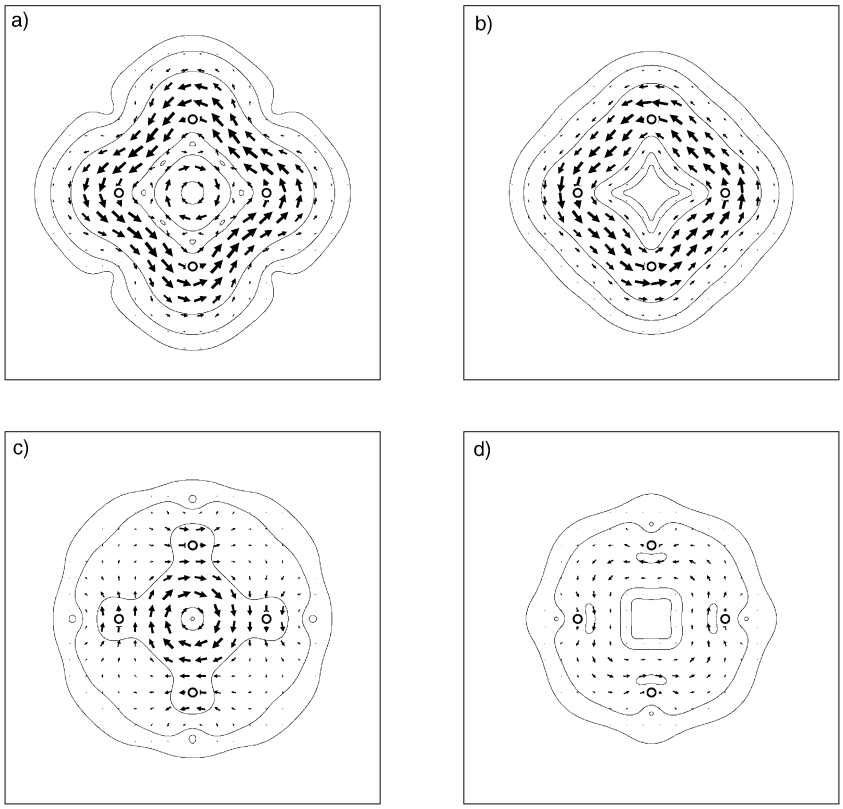

Figure 9. Calculated current-density maps and orbital contributions to ring current for Se_4^{2+} in a plane at a height of $1.5\,a_0$: a) total current density; b) π current density arising from the four electrons of the $5e_g$ HOMO; c) current density arising from the four electrons of the σ $12e_u$ HOMO−1; d) current density arising from the two electrons of the σ $4b_{2g}$ HOMO−4.

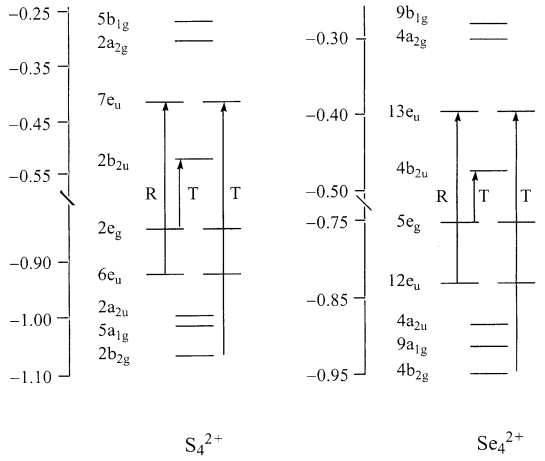

Figure 10. Energy-level diagrams and important translationally (T) and rotationally (R) allowed transitions leading to diatropic and paratropic currents for S_4^{2+} and Se_4^{2+}.

HOMO−4 b_{2g} orbital. The σ orbitals of X_4^{2+} can be qualitatively understood as combinations of four radial lone-pair ($a_{1g} + e_u + b_{1g}$) and four edge-bond ($a_{1g} + e_u + b_{2g}$) localised orbitals, and, as Figure 12 shows, the e_u molecular orbitals responsible for the paratropic σ current are the antibonding combinations of the e_u lone-pair and edge-bond localised functions. The σ molecular orbital responsible for the diatropic current is the antibonding combination of edge bonds. The opposite sense of the two σ orbital currents is compatible with the selection rules for transitions to the σ* LUMO+1 (e_u): $b_{2g} \times e_u = e_u$ (translational) and $e_u \times a_{2g} = e_u$ (rotational). The presence of the diatropic π current density accounts for the negative NICS(1) values for these two molecules (Table 1).

The calculated current-density maps for S_2N_2 (Figure 13) show strong similarities with those of the more symmetrical X_4^{2+} systems. Again there is a 4e diatropic π current arising from the HOMO and HOMO−1 ($1b_{1g}$ and $2b_{2g}$ in D_{2h}), and

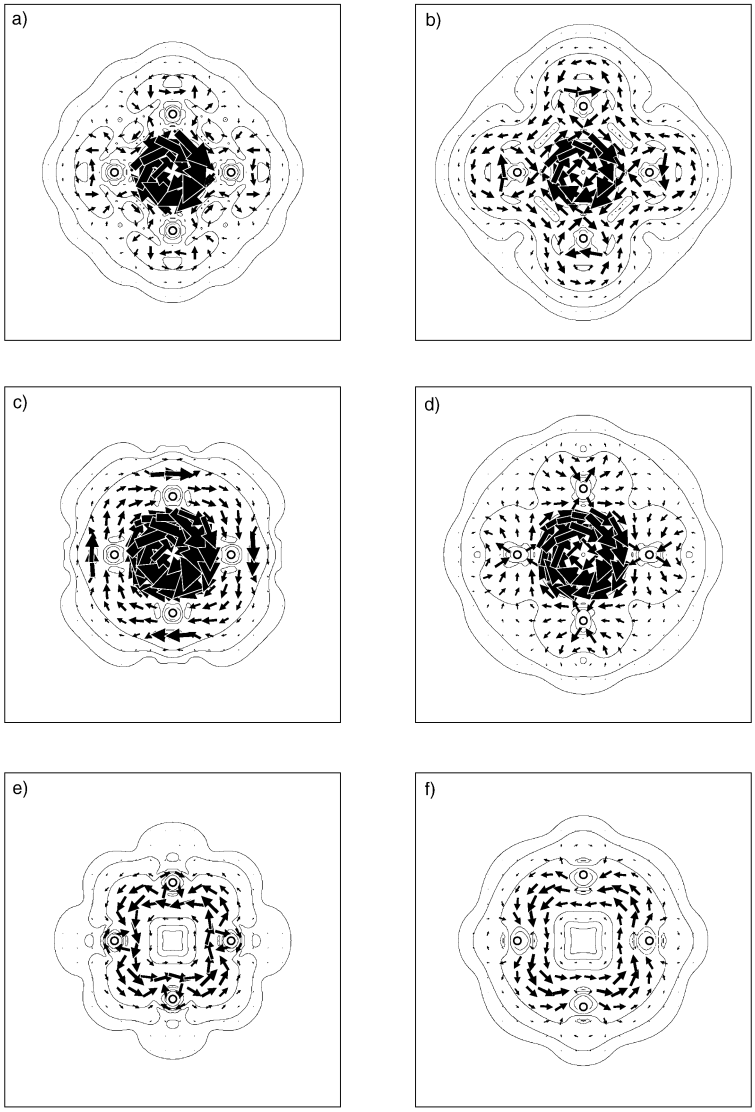

Figure 11. Calculated current-density maps and orbital contributions to ring current for S_4^{2+} and Se_4^{2+} in the molecular plane: a) total current density (S_4^{2+}); b) total current density (Se_4^{2+}); c) current density arising from the four electrons of the σ $6e_u$ HOMO−1 (S_4^{2+}); d) current density arising from the four electrons of the σ $12e_u$ HOMO−1 (Se_4^{2+}); e) current density arising from the two electrons of the σ $2b_{2g}$ HOMO−4 (S_4^{2+}); f) current density arising from the two electrons of the σ $4b_{2g}$ HOMO−4 (Se_4^{2+}).

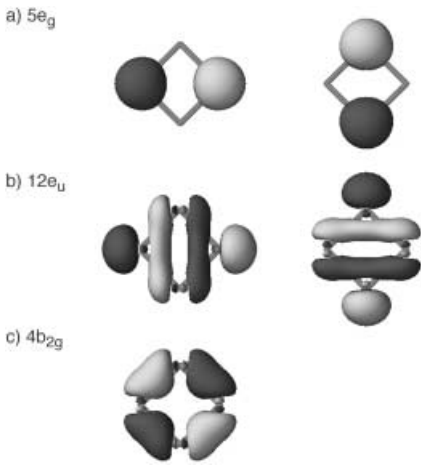

Figure 12. Orbitals with significant contributions to the current-density maps of Se_4^{2+}: a) $5e_g$ HOMO; b) $12e_u$ HOMO−1 c) $4b_{2g}$ HOMO−4.

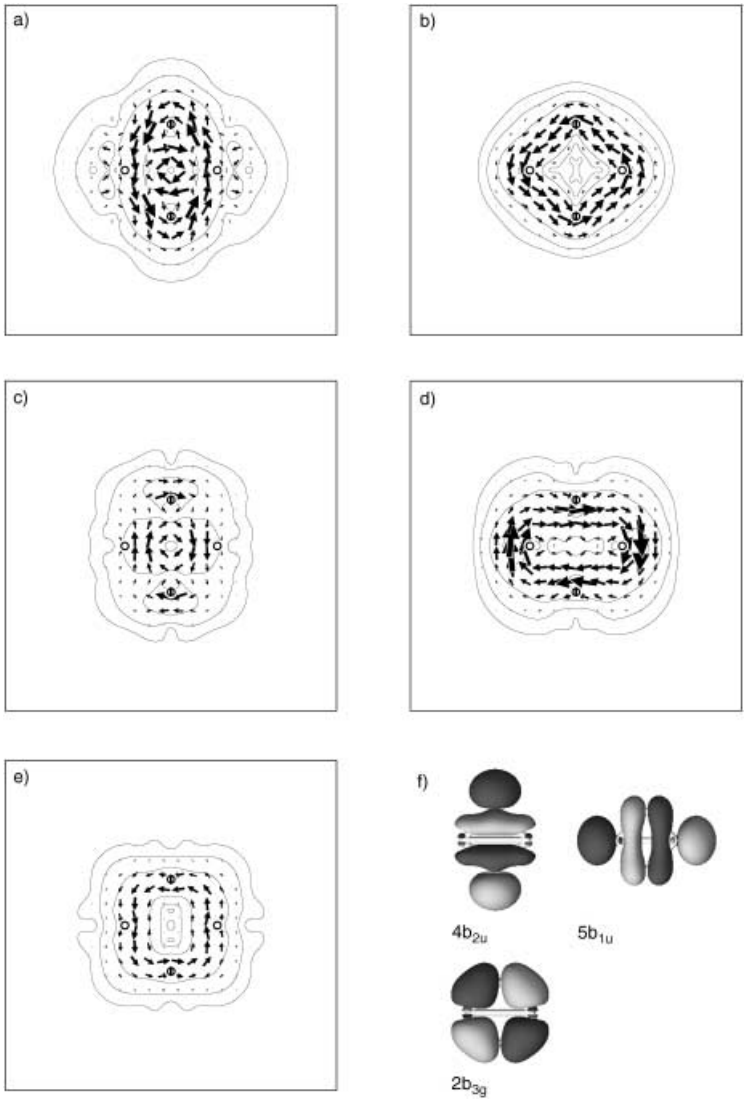

Figure 13. Calculated current-density maps and orbital contributions to ring current for S_2N_2 in a plane at a height of $1.0\,a_0$: a) total current density; b) total π current density; c) current density arising from the two electrons of the σ $4b_{2u}$ HOMO−2; d) current density arising from the two electrons of the σ $5b_{1u}$ HOMO−3; e) current density arising from the two electrons of the σ $2b_{3g}$ HOMO−6; f) the three σ orbitals that make significant contributions to the current-density maps of S_2N_2, displayed with respect to the short S–S nonbonding contact (2.359 Å, B3LYP/6-311+G**).

in the π plotting plane at $1\,a_0$ above the nuclei, there is again a net paratropic contribution from six electrons in high-lying σ orbitals. This σ contribution is made up of a paratropic current from $4b_{2u}$ (HOMO−2) and $5b_{1u}$ (HOMO−3), and a diatropic current from $2b_{3g}$ (HOMO−6).

Unlike the previous examples, the current-density maps for the X_4^{2+} and S_2N_2 systems do not yield a clear-cut answer to the question of aromaticity, as their current is not a simple circulation. From the π current alone, these systems are apparently aromatic; from the σ current alone, they are apparently antiaromatic. The "aromaticity" of the whole current-density distribution is then equivocal, and would depend on which property was used to sample it. The small negative values of NICS(0) and NICS(1) (Table 1) suggest a near cancellation of σ and π effects.

Conclusion

This survey of some simple inorganic monocycles shows that such systems can exhibit diatropic π ring currents and resemble the archetypal π-isoelectronic aromatic [*n*]annulenes. In both the inorganic and organic series, the σ electron contributions, especially in the ring planes, can be large (especially in four-membered rings) and may oppose the π current. The diagnosis of aromaticity on the basis of the ipsocentric ring-current criterion for the systems with larger rings is clear. The 6π-electron P_5^- and As_5^- five-membered rings, akin to N_5^- and the cyclopentadienyl anion, the 10π-electron $S_3N_3^-$, $S_4N_3^-$ and $S_4N_4^{2+}$ systems, akin to the $C_8H_8^{2-}$ dianion, and the 14π-electron $S_5N_5^+$ ring in its planar form are examples thereof. The number of participating electrons and sense of the π current, as shown by the ipsocentric model, follow simple Hückel considerations. The NICS analysis agrees with the main conclusions drawn from the detailed current-density maps. The connection between the clearly defined physical magnetic aromaticity criteria and the chemical properties of such a wide range of systems is necessarily a more complex question and could be a subject for future research.

Acknowledgment

This work was supported in the UK by EU TMR Network grant CT970192, in Belgium by The Fund for Scientific Research-Flanders (Belgium) and in the USA by National Science Foundation Grant CHE-0209857.

[1] a) A. Streitwieser Jr. , *Molecular Orbital Theory for Organic Chemists*, Wiley, New York, **1961**; b) P. J. Garratt, *Aromaticity*, McGraw-Hill, London, **1971**; c) V. I. Minkin, M. N. Glukhovtsev, B. Y. Simkin, *Aromaticity and Antiaromaticity. Electronic and Structural Aspects*, Wiley, New York, **1994**; d) M. B. Smith, J. March, *March's Advanced Organic Chemistry: Reactions, Mechanisms and Structure*, 5th Ed., Wiley New York, **2001**; e) For recent reviews on many aspects, see: *Chem. Rev.* **2001**, *101*, 1349–1566 (Special Issue on Aromaticity, P. von R. Schleyer, Guest Editor).

[2] a) T. M. Krygowski, M. K. Cyranski, Z. Czarnocki, G. Hafelinger, A. R. Katritzky, *Tetrahedron* **2000**, *56*, 1783–1796; b) M. K. Cyranski, T. M. Krygowski, A. R. Katritzky, P. von R. Schleyer, *J. Org. Chem.* **2002**, *67*, 1333–1338.

[3] a) J. A. Elvidge, L. M. Jackman, *J. Chem. Soc.* **1961**, 859–866; b) P. von R. Schleyer, H. Jiao, *Pure. Appl. Chem.* **1996**, *68*, 209–218;

[4] a) P. von R. Schleyer, C. Maerker, A. Dransfeld, H. Jiao, N. J. R. van Eikema Hommes, *J. Am. Chem. Soc.* **1996**, *118*, 6317–6318; b) P. von R. Schleyer, H. Jiao, N. J. R. van Eikema Hommes, V. G. Malkin, O. L. Malkina, *J. Am. Chem. Soc.* **1997**, *119*, 12669–12670.

[5] a) T. M. Krygowski, M. K. Cyranski, *Chem. Rev.* **2001**, *101*, 1385–1419; b) M. K. Cyranski, P. von R. Schleyer, T. M. Krygowski, H. Jiao, G. Hohlneicher, *Tetrahedron* **2003**, *59*, 1657–1665; c) F. De - Proft, P. Geerlings, *Chem. Rev.* **2001**, *101*, 1451–1464; d) P. Geerlings, F. De Proft, W. Langenaeker, *Chem. Rev.* **2003**, *103*, 1793–1873.

[6] a) See for example: B. Kiran, A. K. Phukan, E. D. Jemmis, *Inorg. Chem.* **2001**, *40*, 3615–3618, and references therein; b) P. von R. Schleyer, K. Najafian, *Inorg. Chem.* **1998**, *37*, 3455–3470; c) R. B. King, *Chem. Rev.* **2001**, *101*, 1119–1152; d) H. J. Zhai, L. S. Wang, A. E. Kuznetsov, A. I. Boldyrev, *J. Phys. Chem. A.* **2002**, *106*, 5600–5606.

[7] X. Li, A. E. Kuznetsov, H.-F. Zhang, A. I. Boldyrev, L.-S. Wang, *Science* **2001**, *291*, 859–861.

[8] a) T. A. Keith, R. F. W. Bader, *Chem. Phys. Lett.* **1993**, *210*, 223–231; b) T. A. Keith, R. F. W. Bader, *J. Chem. Phys.* **1993**, *99*, 3669–3682; c) R. Zanasi, P Lazzeretti, M. Malagoli, F. Piccinini, *J. Chem. Phys.* **1995**, *102*, 7150–7157; d) R. Zanasi, *J. Chem. Phys.* **1996**, *105*,1460–1469.

[9] a) P. W. Fowler, E. Steiner, *J. Phys. Chem. A* **1997**, *101*, 1409–1413; b) E. Steiner, P. W. Fowler, *Int. J. Quantum Chem.* **1996**, *60*, 609–616; c) E. Steiner, P. W. Fowler, *Chem. Commun.* **2001**, 2220–2221; d) E. Steiner, P. W. Fowler, *J. Phys. Chem. A* **2001**, *105*, 9553–9562; e) P. W. Fowler, E. Steiner, R. Zanasi, B. Cadioli, *Mol. Phys.* **1999**, *96*, 1099–1108; f) E. Steiner, P. W. Fowler, L. W. Jenneskens, *Angew. Chem.* **2001**, *113*, 375–379; *Angew. Chem. Int. Ed.* **2001**, *40*, 362–366, and references therein.

[10] a) P. W. Fowler, R. W. A. Havenith, E. Steiner, *Chem. Phys. Lett.* **2001**, *342*, 85–90; b) P. W. Fowler, R. W. A. Havenith, E. Steiner, *Chem. Phys. Lett.* **2002**, *359*, 530–536.

[11] a) For discussions of the compounds studied here, see, for example: N. N. Greenwood, A. Earnshaw, *Chemistry of the Elements*, Butterworth-Heineman, Oxford, **2001**; F. A. Cotton, G. Wilkinson, C. A. Murillo, M. Bochmann, *Advanced Inorganic Chemistry*, Sixth Edition, Wiley, New York, **1999**; b) O. J. Scherer, *Angew. Chem.* **1990**, *102*, 1137–1155; *Angew. Chem. Int. Ed. Engl.* **1990**, *29*, 1104–1122; O. J. Scherer, *Acc. Chem. Res.* **1999**, *32*, 751–762; c) M. Baudler, D. Duster, D. Ouzounis, *Z. Anorg. Allg. Chem.* **1987**, *544*, 87–94; M. Baudler, S. Akpapoglou, D. Ouzounis, F. Wasgestian, B. Meinigke, H. Budzikiewiz, H. Munster, *Angew. Chem.* **1988**, *100*, 288–289; *Angew. Chem. Int. Ed. Engl.* **1988**, *27*, 280–281; M. Baudler, T. Etzbach, *Chem. Ber.* **1991**, *124*, 1159–1160; d) O. J. Scherer, T. Bruck, *Angew. Chem.* **1987**, *99*, 59–59; *Angew. Chem. Int. Ed. Engl.* **1987**, *26*, 59–59; O. J. Scherer, J. Schwalb, G. Wolmershauser, W. Kaim, R. Gross, *Angew. Chem.* **1986**, *98*, 349–350; *Angew. Chem. Int. Ed. Engl.* **1986**, *25*, 363–364; J. A. Chamizo, M. Ruizmazon, R. Salcedo, R. A. Toscano, *Inorg. Chem.* **1990**, *29*, 879–880; e) E. Urnezius, W. W. Brennessel, C. J. Cramer, J. E. Ellis, P. von R. Schleyer, *Science* **2002**, *295*, 832–834; f) A. L. Rheingold, M. J. Foley, P. J. Sullivan, *J. Am. Chem. Soc.* **1982**, *104*, 4727–4729; g) E. J. Malar, *J. Org. Chem.* **1992**, *57*, 3694–3698; A. Dransfeld, L. Nyulaszi, P. von R. Schleyer, *Inorg. Chem.* **1998**, *37*, 4413–4420; h) T. Chivers, *Chem. Rev.* **1985**, *85*, 341–365; i) J. Bojes, T. Chivers, W. G. Laidlaw, M. Trsic, *J. Am. Chem. Soc.* **1979**, *101*, 4517–4522; R. Jones, P. F. Kelly, D. J. Williams, J. D. Woollins, *Polyhedron* **1987**, *6*, 1541–1545; P. N. Jagg, P. F. Kelly, H. S. Rzepa, D. J. Williams, J. D. Woollins, W. Wylie, *J. Chem. Soc. Chem. Commun.* **1991**, 942–944; j) R. J. Gillespie, D. R. Slim, J. D. Tyrer, *J. Chem. Soc. Chem. Commun.* **1977**, 253–255; R. J. Gillespie, J. P. Kent, J. F. Sawyer, D. R. Slim, J. D. Tyrer, *Inorg. Chem.* **1981**, *20*, 3799–3812; k) A. J. Banister, Z. V. Hauptman, A. G. Kendrick, *J. Chem. Soc. Dalton Trans.* **1987**, 915–924; l) R. J. Gillespie *Chem. Soc. Rev*, **1979**, *8*, 315–352; J. Beck, *Coord. Chem. Rev.* **1997**, *163*, 55–70; R. C. Burns, R. J. Gillespie, *Inorg. Chem.* **1982**, *21*, 3877–3886.

[12] a) D. Moran, M. Manoharan, T. Heine, P. von R. Schleyer, *Org. Lett.* **2003**, *5*, 23–26, and references therein; b) P. von R. Schleyer, M. Manoharan, Z.-X. Wang, B. Kiran, H. Jiao, R. Puchta, N. J. R. van Eikema Hommes, *Org. Lett.* **2001**, *3*, 2465–2468.

[13] Gaussian 98, Revision A.9, M. J. Frisch, G. W. Trucks, H. B. Schlegel, G. E. Scuseria, M. A. Robb, J. R. Cheeseman, V. G. Zakrzewski, J. A. Montgomery, Jr., R. E. Stratmann, J. C. Burant, S. Dapprich, J. M. Millam, A. D. Daniels, K. N. Kudin, M. C. Strain, O. Farkas, J. Tomasi, V. Barone, M. Cossi, R. Cammi, B. Mennucci, C. Pomelli, C. Adamo, S. Clifford, J. Ochterski, G. A. Petersson, P. Y. Ayala, Q. Cui, K. Morokuma, D. K. Malick, A. D. Rabuck, K. Raghavachari, J. B. Foresman, J. Cioslowski, J. V. Ortiz, A. G. Baboul, B. B. Stefanov, G. Liu, A. Liashenko, P. Piskorz, I. Komaromi, R. Gomperts, R. L. Martin, D. J. Fox, T. Keith, M. A. Al-Laham, C. Y. Peng, A. Nanayakkara, M. Challacombe, P. M. W. Gill, B. Johnson, W. Chen, M. W. Wong, J. L. Andres, C. Gonzalez, M. Head-Gordon, E. S. Replogle, J. A. Pople, Gaussian, Inc., Pittsburgh PA, **1998**.

[14] P. Lazzeretti, R. Zanasi, SYSMO package (University of Modena), **1980**. Some additional routines for the evaluation and plotting of current density, orbital analysis and localisation were written in Exeter (E. Steiner, P. W. Fowler, R. W. A. Havenith).

[15] a) L. Nyulaszi, P. von R. Schleyer, *J. Am. Chem. Soc.* **1999**, *121*, 6872–6875; See: b) P. von R. Schleyer, P. K. Freeman, H. Jiao, B. Goldfuss, *Angew. Chem.* **1995**, *107*, 332–335; *Angew. Chem. Int. Ed. Eng.* **1995**, *34*, 337–340; F. Pühlhofer, R. Sauers, O. Charkin, N. Klimenko, P. von R. Schleyer, in preparation.

[16] J. Pipek, P. G. Mezey, *J. Chem. Phys.* **1989**, *90*, 4916–4926.

[17] a) V. G. Malkin, O. L. Malkina, M. E. Casida, D. R. Salahub, *J. Am. Chem. Soc.* **1994**, *116*, 5898–5908; b) V. G. Malkin, O. L. Malkina, L. A. Eriksson, D. R. Salahub in *Modern Density Functional Theory* (Eds.: J. M. Seminario, P. Politzer), Elsevier, Amsterdam, **1995**, pp. 273–347.

[18] a) J. P. Perdew in *Electronic Structure of Solids* (Eds.: P. Ziesche, H. Eschrig), Akademie Verlag, Berlin, **1991**; b) J. P. Perdew, Y. Wang, *Phys. Rev. B* **1992**, *45*, 13244–13249.

[19] W. Kutzelnigg, U. Fleischer, M. Schindler in *NMR-Basic Principles and Progress, Vol. 23*, Springer, Heidelberg, **1990**, p. 165.

Received: June 30, 2003
Revised: October 29, 2003 [F5291]